Dynamical SU(3) Linear σ Model and the mixing of η'–η and σ–f_0 mesons

D. Kekez[a], D. Klabučar[b], M. D. Scadron[c]

[a] *Rudjer Bošković Institute, P.O.B. 180, 10001 Zagreb, Croatia*

[b] *Physics Department, Faculty of Science, University of Zagreb, Bijenička c. 32, Zagreb 10000, Croatia*

[c] *Physics Department, University of Arizona, Tucson Az 85721 USA*

Abstract

The SU(3) linear σ model ($L\sigma M$) is dynamically generated in loop-order using the nonstrange–strange basis. Only self–consistent logarithmic divergent graphs are needed, with quadratic divergent graphs replaced by SU(3) mass-shell equal splitting laws. The latter lead to an η'–η mixing angle of 41.84^0 which is consistent with phenomenology. Finally this above SU(3)$L\sigma M$ in turn predicts strong decay rates which are all compatible with data.

Preprint submitted to Elsevier Preprint *29 October 2018*

1 Introduction

The original tree–level SU(2) spontaneous symmetry breaking (SSB) linear σ model ($L\sigma M$) interaction Lagrangian density is [1]

$$L^{\rm int}_{L\sigma M} = g\bar{\psi}\left(\sigma + i\gamma_5 \boldsymbol{\tau}\cdot\boldsymbol{\pi}\right)\psi + g'\sigma(\sigma^2+\boldsymbol{\pi}^2) - \frac{\lambda}{4}(\sigma^2+\boldsymbol{\pi}^2)^2 \ , \tag{1}$$

with tree–order chiral limiting (CL) couplings satisfying for $f_\pi \approx 93$ MeV

$$g = \frac{m}{f_\pi}, \quad g' = \frac{m_\sigma^2}{2f_\pi} = \lambda f_\pi \ , \tag{2}$$

here for quark fields, constituent quark mass m and cubic and quartic–meson couplings g', λ. Although the g, g', λ in (2) are not further specified in tree order, in loop order they are dynamically generated as

$$g = \frac{2\pi}{\sqrt{3}} \approx 3.6276 \ , \quad g' = 2gm \approx 2.3 \text{ GeV} \ , \quad \lambda = \frac{8\pi^2}{3} \approx 26.3 \, . \tag{3}$$

We take $m = 315$ MeV, i.e., roughly one third of the nucleon mass M_N, since this value most consistently satisfies the relations central for the present paper, namely mass shell equal splitting laws (MSESLs) considered below, in Sec. 3. (A dynamical quark mass $m = \left[\frac{4\pi\alpha_s}{3}\langle -\bar{\psi}\psi\rangle_{1\rm GeV}\right]^{1/3} \approx 320$ MeV used in QCD [2] would lead to some 3% higher MSESLs value $4m^2$, whereas $m = 325$ MeV, used in Refs. [3], would lead to some 6% higher value.) While Refs. [3] recover the original chiral relations of Eqs. (2), the loop–order values in Eqs. (3) depend on relating slowly diverging log–divergent graphs with the more rapidly diverging quadratic–divergent graphs.

In this paper we instead dynamically generate the SU(3) $L\sigma M$ using only the log–divergent graphs while replacing the quadratic–divergent graphs with the dynamical SU(3) MSESLs. In Sec. 2 we review the log–divergent gap equations in the CL and show their self–consistency in loop order. Then in Sec. 3 we replace quadratic–divergent mass gap equations with SU(2) and SU(3) MSESLs. In Sec. 4 we show how the SU(3) MSESLs lead to an η–η' nonstrange–strange mixing angle of $\sim 42^0$, in fact closely agreeing with the phenomenological value [4,5]. Finally in Sec. 5 we employ this SU(3) $L\sigma M$ with nonstrange–strange η, η' couplings to predict strong interaction decay rates for $\sigma_{NS} \to \pi\pi$, $a_0 \to \eta\pi$, $f_0 \to \pi\pi$ and $\eta' \to \eta\pi\pi$, all in close agreement with data [6]. We give our conclusions in Sec. 6.

2 Self–consistent log divergent gap equations

We begin with the non–perturbative loop–order equation for the pion decay constant $\delta f_\pi = f_\pi$ in the soft–pion chiral limit [3]:

$$1 = -i\, 4N_c\, g^2 \int \frac{\bar{d}^4 p}{(p^2 - m^2)^2}\,, \tag{4}$$

using the Goldberger–Treiman relation (GTR) $m = f_\pi g$ as in (2) with $\bar{d}^4 p = (2\pi)^{-4} d^4 p$, where the quark mass m cancels out of this gap Eq. (4). This log–divergent gap equation (LDGE) (4) with $g \sim 315$ MeV/90 MeV ~ 3.5 requires an ultraviolet cutoff $\Lambda \approx 750$ MeV, separating the $\overline{q}q$ elementary particles π and $m_\sigma \sim 650$ MeV [6] with $m_{\pi,\sigma} < \Lambda$ from the bound-state $\overline{q}q$ mesons $\Lambda < \rho(770)$, $\omega(780)$, $a_1(1260)$. This natural separation of $L\sigma M$ elementary particles from bound states is a consequence of the $Z = 0$ compositeness condition [7] $g = 2\pi/\sqrt{N_c}$ or $g = 3.6276$ for $N_c = 3$ (also dynamically generated in Refs. [3]).

The self–consistency of loops "shrinking" to trees in the CL and their link to the LDGE are seen for quark triangle and quark box graphs. In the former case the quark triangle representing $g'_{\sigma\pi\pi}$ is log–divergent with

$$g'_{\sigma\pi\pi} = -8ig^3 N_c m \int \frac{\bar{d}^4 p}{(p^2 - m^2)^2} = 2gm \left[-4iN_c g^2 \int \frac{\bar{d}^4 p}{(p^2 - m^2)^2} \right] = 2gm\,, \tag{5}$$

by virtue of the LDGE (4). Then using the quark–level GTR, Eq. (5) shrinks to the tree level $g'_{\sigma\pi\pi} \to g' = m_\sigma^2/2f_\pi$ of (2) *provided* that $m_\sigma = 2m$, the Nambu-Jona-Lasino [8] (NJL) result also dynamically generated in Refs. [3]. Likewise the $\pi\pi$ box graph in the CL gives the quartic quark coupling [3]

$$\lambda_{\rm box} = -8iN_c\, g^4 \int \frac{\bar{d}^4 p}{(p^2 - m^2)^2} = 2g^2 \left[-4iN_c\, g^2 \int \frac{\bar{d}^4 p}{(p^2 - m^2)^2} \right] = 2g^2\,, \tag{6}$$

again via the LDGE (4). Then using the GTR, Eq. (6) becomes

$$\lambda_{\rm box} \;= 2g^2 = \frac{2gm}{f_\pi} = \frac{g'}{f_\pi} = \lambda_{\rm tree} \tag{7}$$

by virtue of the tree–level $L\sigma M$ couplings in Eq. (2). So again loops shrink to trees, while recovering the NJL scalar mass $m_\sigma = 2m$ in this self–consistent fashion [3].

Next the CL quark bubble plus quark σ tadpole graphs, although both being quadratically divergent give a *vanishing* $m_\pi^2 = 0$ in the CL (as required) provided the couplings

satisfy $g'_{\sigma\pi\pi} = m_\sigma^2/2f_\pi$, again recovering Eq. (2), but independent of the quadratically divergent scale.

Lastly the pion quark triangle photon graph automatically normalizes the form factor $F_\pi(q^2=0)=1$ as expected. Specifically this quark triangle predicts [9]

$$F_\pi(q^2) = -i\,4N_c\,g^2 \int_0^1 dx \int \frac{\bar{d}^4p}{[p^2 - m^2 + x(1-x)q^2]^2} \ ,$$

recovering $F_\pi(q^2=0)=1$ due to the LDGE (4).

3 Mass–Shell Equal Splitting Laws

To continue circumventing the dangerous quadratic divergent tadpole graphs, we first invoke the Lee null tadpole sum [10] characterizing the true (not false SSB) vacuum. Using only dimensional analysis, the vanishing tadpole sum requires [3] $N_c(2m)^4 = 3m_\sigma^4$, or $N_c = 3$ for the SU(2) $L\sigma M$ since we already know from Sec. 2 that the NJL relation $m_\sigma = 2m$ is also valid in the $L\sigma M$ in the CL, as is $g = 2\pi/\sqrt{3}$ [7].

Away from the CL this NJL condition becomes for $m \approx M_N/3 \approx 315$ MeV,

$$m_\sigma^2 - m_\pi^2 = 4m^2 \approx 0.397 \text{ GeV}^2 \ . \tag{8}$$

In Sec. 4 we will show that η'–η mixing requires a nonstrange–strange (NS–S) mixing angle $\phi_P \approx 41.84^0$, which in turn fixes the eta NS mass to be $m_{NS} = 757.9$ MeV. Then the SU(3) extension of the mass-shell equal splitting law (MSESL) Eq. (8) is for $m_{a_0} \approx 984.8$ MeV,

$$m_{a_0}^2 - m_{\eta_{NS}}^2 \approx 0.395 \text{ GeV}^2 \ , \tag{9}$$

which we again identify with the NS quark mass factor $4m^2$ in Eq. (8).

MSESL (9) follows from the empirical $m_{a_0}^2$ and from $m_{\eta_{NS}}^2$ extracted in a phenomenological way in Sec. 4 (see also Ref. [11]), but we have yet another way to avoid quadratic divergent amplitudes and evaluate the difference of the a_0 and η_{NS} self-energies explicitly. It is encouraging that this explicit calculation below yields results which are reasonably close to MSESL (9), even though we consider only the lowest-order $L\sigma M$ self-energy graphs. Also, in counterdistinction to Eq. (9) [1], these graphs do not capture (at least not

[1] In Eq. (9), we plug in $m_{NS} = 757.9$ MeV which *does* contain [11] the shift due to the gluon anomaly.

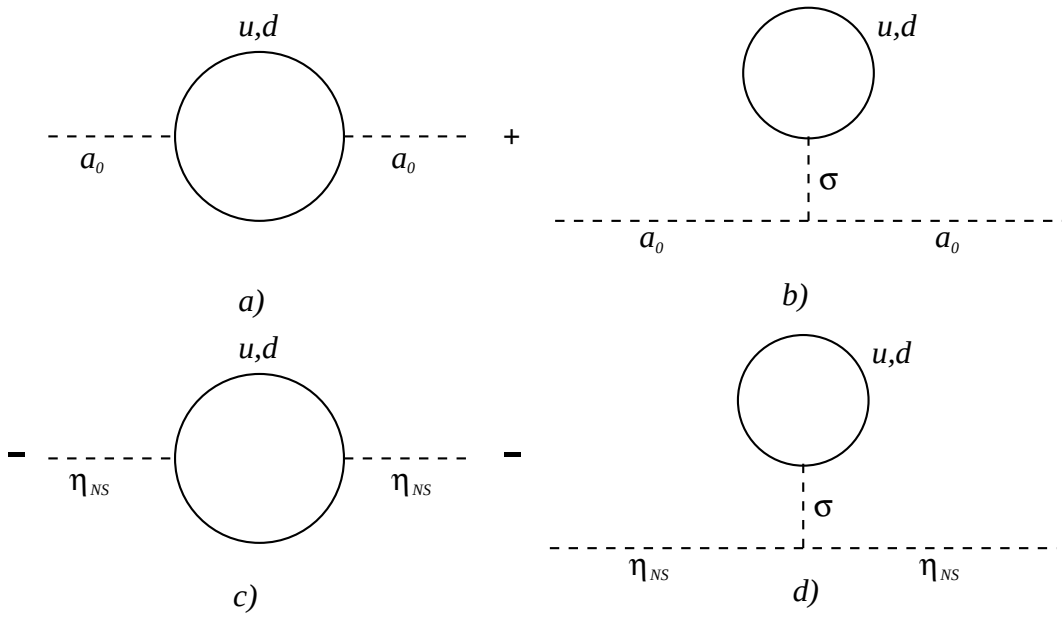

Fig. 1. Bubble graphs and tadpole graphs

fully) the effect of the gluon anomaly which influences strongly the masses in the $\eta - \eta'$ complex.

This other way to avoid quadratic divergent amplitudes is to subtract mass shell bubble (and tadpole) graphs of Fig. 1. Since the quadratic divergent tadpole graphs of Figs. 1 b,d clearly cancel (due to the $L\sigma M$ coupling relation $g'_{a_0 a_0 \sigma} = g'_{\eta_{NS}\eta_{NS}\sigma}$), the remaining quadratically divergent bubble graph difference (Figs. 1 a,c) give the formal result

$$m^2_{a_0} - m^2_{\eta_{NS}} = -8iN_c\, g^2 \int_0^1 dx \int \bar{d}^4p \left[\frac{p^2 - m^2_{a_0} x(1-x) + m^2}{(p^2 + m^2_{a_0} x(1-x) - m^2)^2} - \frac{p^2 - m^2_{\eta_{NS}} x(1-x) - m^2}{(p^2 + m^2_{\eta_{NS}} x(1-x) - m^2)^2} \right] . \tag{10}$$

Here we have combined propagator denominators using Feynman's trick

$$\frac{1}{ab} = \int_0^1 \frac{dx}{[ax + b(1-x)]^2} .$$

In other words, we evaluate the bubble graphs with propagator momentum $p \to p - qx$ for mass shell values $q^2 = m^2_{a_0}$, $m^2_{\eta_{NS}}$ for Figs. 1 a, c. Specifically for $m_{a_0} = 984.8$ MeV and $m_{\eta_{NS}} = 757.9$ MeV and a constituent nonstrange quark mass of 315 MeV, a computer calculation detailed in the Appendix, evaluates Eq. (10) as

$$m^2_{a_0} - m^2_{\eta_{NS}} = 5.83\, m^2 - i\, 3.83\, m^2 . \tag{11}$$

We neglect the negative imaginary part of Eq. (11) (compatible with unitarity) since quarks in the bubble graph of Figs. 1 should be confined. Considering the delicate cancellation due to the mean value ($6\int_0^1 x(1-x)=1$) giving in the second denominator in Eq. (10) $m^2_{\eta_{NS}}x(1-x)-m^2 \approx -0.035\,m^2$, and especially recalling *i)* that we have used only the lowest order graphs and *ii)* that it is known that the gluon anomaly shifts $m_{\eta_{NS}}$ upwards [which is taken into account in the result (11) only partially and indirectly, through the mass shell value $q^2=m^2_{\eta_{NS}}=(757.9\ \mathrm{MeV})^2$] so that the difference (11) is understandably somewhat overestimated, we suggest that the real part of (11) is not far from the numerical values of Eqs. (8) and (9), i.e. [12],

$$m^2_{\sigma_{NS}}-m^2_\pi = m^2_{a_0}-m^2_{\eta_{NS}} = 4m^2 \approx 0.397\ \mathrm{GeV}^2\ . \tag{12}$$

Stated another way, combining the partial fraction integrands in Eq. (10), we note that the leading p^6 terms in the numerator of (10) exactly cancel since they are quadratically divergent terms. Moreover, the log–divergent p^4 terms in (10) are proportional to $6(m^2_{a_0}-m^2_{\eta_{NS}})x(1-x)-m^2$; they cancel using the mean value, resulting in $m^2_{a_0}-m^2_{\eta_{NS}}=4m^2$. Thus again we support the MSESLs of Eq. (12).

4 Dynamical η'–η Mixing

Given the MSESL Eq. (12), one may extract the NS eta mass as $m_{\eta_{NS}} \approx 757$ MeV. Alternatively we may express the eta NS–S mass matrix as

$$\begin{bmatrix} m^2_{\eta_{NS}} & \gamma \\ \gamma & m^2_{\eta_S} \end{bmatrix} \underset{\phi_P}{\rightarrow} \begin{bmatrix} m^2_\eta & 0 \\ 0 & m^2_{\eta'} \end{bmatrix}\ , \tag{13}$$

where the NS–S pseudoscalar mixing angle ϕ_P determines the mixing relations

$$|\eta\rangle = \cos\phi_P|\eta_{\mathrm{NS}}\rangle - \sin\phi_P|\eta_{\mathrm{S}}\rangle\ , \quad |\eta'\rangle = \sin\phi_P|\eta_{\mathrm{NS}}\rangle + \cos\phi_P|\eta_{\mathrm{S}}\rangle\ . \tag{14}$$

The angle ϕ_P is uniquely determined via the trace constraint

$$m^2_{\eta_{NS}}+m^2_{\eta_S} = m^2_\eta + m^2_{\eta'} \approx 1.217\ \mathrm{GeV}^2\ , \tag{15}$$

(because the diagonal masses m_η and $m_{\eta'}$ are measured [6]) with off–diagonal hamiltonian matrix elements vanishing $\langle\eta'|H|\eta\rangle = \langle\eta|H|\eta'\rangle = 0$, giving

$$m^2_{\eta_{NS}} = \cos^2\phi_P\, m^2_\eta + \sin^2\phi_P\, m^2_{\eta'}\ , \quad m^2_{\eta_S} = \sin^2\phi_P\, m^2_\eta + \cos^2\phi_P\, m^2_{\eta'}\ . \tag{16}$$

The two–level quantum mechanical solution of Eqs. (13), (15), (16) is the angle

$$\phi_P = \arctan\sqrt{\frac{m^2_{\eta_{NS}} - m^2_\eta}{m^2_{\eta'} - m^2_{\eta_{NS}}}} = 41.84^0 \ , \tag{17}$$

with masses

$$m_{\eta_{NS}} = 757.9 \text{ MeV} \ , \quad m_{\eta_S} = 801.5 \text{ MeV} \ . \tag{18}$$

Not only is the eta NS mass in (18) close to 757 MeV found via the MSESL Eq. (12), but the mixing angle in (17) is precisely the dynamical angle obtained via nonperturbative QCD. More specifically, Refs. [13,11] predict ϕ_P as

$$\phi_P = \arctan\sqrt{\frac{(m^2_{\eta'} - 2m^2_K + m^2_\pi)(m^2_\eta - m^2_\pi)}{(2m^2_K - m^2_\pi - m^2_\eta)(m^2_{\eta'} - m^2_\pi)}} = 41.84^0 \ , \tag{19}$$

found from the nonperturbative QCD gluon quark annihilation strength

$$\beta = \frac{(m^2_{\eta'} - m^2_\pi)(m^2_\eta - m^2_\pi)}{4(m^2_K - m^2_\pi)} \approx 0.278 \text{ GeV}^2 \tag{20}$$

and a constituent quark mass ratio $X \approx 0.78 \approx \hat{m}/m_s$ obtained from the NS–S QCD mass matrix [13,11]

$$\begin{bmatrix} m^2_\pi + 2\beta & \sqrt{2}\beta X \\ \sqrt{2}\beta X & 2m^2_K - m^2_\pi + \beta X^2 \end{bmatrix} \underset{\phi_P}{\rightarrow} \begin{bmatrix} m^2_\eta & 0 \\ 0 & m^2_{\eta'} \end{bmatrix} \ . \tag{21}$$

Equations (18), (20), (21) have the solution

$$\tan(2\phi_P) = 2\sqrt{2}\beta X (m^2_{\eta_S} - m^2_{\eta_{NS}})^{-1} = 9.02 \text{ or } \phi_P = 41.84^0 \ . \tag{22}$$

Again we see that ϕ_P in (17), (19) and (22) are extremely close in magnitude. Moreover, the dynamical approach to η–η' using the Schwinger–Dyson (SD) and Bethe–Salpeter (BS) integral equations found $\phi_P \approx 42^0$ (that is, in terms of the singlet–octet state mixing angle $\theta_P \equiv \phi_P - \arctan\sqrt{2} \approx -12.7^0$) [14]. Its subsequent refinement [11] also included the effect of the "strangeness attenuation parameter" X in the SD–BS mass matrix. The SD–BS estimate was $X = 0.663$, again close to the constituent quark mass ratio $\hat{m}/m_s$ found there. Fitting the trace constraint (15) then led to $\beta = 0.277$ GeV^2, practically the same as Eq. (20), to $m_{\eta_{NS}} = 757.87$ MeV and $m_{\eta_S} = 801.45$ MeV, almost the same as Eq. (18), and to $\theta_P = -13.4^0$, that is, $\phi_P = 41.3^0$, very close to ϕ_P in Eq. (22). (These results

were for the original parameters of Ref. [14]. Reference [11] also varied the parameters to check the sensitivity on SD-BS modeling, but the results changed little.) Because of the close link between Eqs. (17), (18), the QCD Eqs. (19), (22) and the SD–BS scheme, we suggest that $\phi_P \approx 41.84^0$ is the dynamical η'–η mixing angle in the NS–S quark basis. It corresponds to [4,5] the singlet–octet angle $\theta_P = \phi_P - \arctan\sqrt{2} \approx -12.9^0$. Also note that Ref. [11] showed there is no contradiction between our approach utilizing one state–mixing angle, and the mixing scheme employing two angles pertaining to the mixing of the decay constants (see Refs. [5], esp. the second reference for review.) Not only is the difference small in the NS-S basis, but our Ref [11] also showed that our results are in agreement with what is found in the two–angle scheme [5].

It is also satisfying that the phenomenological analysis of the NS–S η'–η NS mixing angle extracts [4] $\phi_P = 43.2^\circ \pm 2.8^\circ$ from $T \to PP$ decays, $\phi_P = 36.6^\circ \pm 1.4^\circ$ from $V \to P\gamma$ and $P \to V\gamma$ decays, $\phi_P = 41.3^\circ \pm 1.3^\circ$ from $P \to \gamma\gamma$ decays and $\phi_P = 40.2^\circ \pm 2.8^\circ$ from $J/\psi \to \rho\eta, \rho\eta'$ and $\omega\pi^0$ decays. Moreover the recent Refs. [5] obtain $\phi_P = 39.3^\circ \pm 1.0^\circ$ by global phenomenological fits and $\phi_P = 42.4^\circ$ as their theoretical prediction, which is all within the region of the dynamical ϕ_P angles in Eqs. (17) or (19).

5 SU(3) LσM Strong Decay Rates

We have thus far used the LDGE (4), induced the MSESLs $m^2_{\sigma_{NS}} - m^2_\pi = m^2_{a_0} - m^2_{\eta_{NS}} = m^2_\kappa - m^2_K = 4m^2 \approx 0.397\ \mathrm{GeV}^2$ (for $\kappa(805-820)$ advocated by, e.g., Delbourgo and Scadron [12]) and the NS–S mixing angle $\phi_P \approx 41.84^0$ all while avoiding quadratic divergent graphs and extending the SU(2) $L\sigma M$ to SU(3). In the latter case the cubic meson $L\sigma M$ Lagrangian density has the SU(3) form [12]

$$L^{L\sigma M}_{\rm cubic} = d_{ijk}\left(g'_{SPP}S^iP^jP^k + g'_{SSS}S^iS^jS^k\right)\ . \tag{23}$$

Then with $f_\pi \approx 93$ MeV and $m \approx M_N/3 \approx 315$ MeV, the MSESLs above suggest the Lagrangian g'_{SPP} couplings

$$g'_{\sigma_{NS}\pi\pi} = \frac{m^2_{\sigma_{NS}\pi\pi} - m^2_\pi}{2f_\pi} \approx 2.13\ \mathrm{GeV}\ , \tag{24}$$

$$g'_{a_0\eta_{NS}\pi} = \frac{m^2_{a_0} - m^2_{\eta_{NS}}}{2f_\pi} \approx 2.13\ \mathrm{GeV}\ , \tag{25}$$

$$g'_{\kappa K\pi} = \frac{m^2_\kappa - m^2_K}{2f_\pi} \approx 2.13\ \mathrm{GeV}\ , \tag{26}$$

along with $g'_{a_0\eta\pi} = \cos\phi_P\, g'_{a_0\eta_{NS}\pi}$, $g'_{\eta' a_0\pi} = \sin\phi_P g'_{a_0\eta_{NS}\pi}$, etc.

The nonstrange σ decay rate is predicted as [6,15]

$$\Gamma(\sigma_{NS} \to \pi\pi) = \frac{3}{2}(2g'_{\sigma_{NS}\pi\pi})^2 \frac{|\vec{p}|}{8\pi m^2_{\sigma_{NS}}} \approx 754 \text{ MeV} , \tag{27}$$

for $m_{\sigma_{NS}} \approx 650$ MeV and $|\vec{p}| = 294$ MeV. This rate is compatible with Weinberg's mended chiral symmetry estimate [16]:

$$\Gamma_{\sigma_{NS}} \approx \frac{9}{2}\Gamma_\rho \approx 676 \text{ MeV} . \tag{28}$$

Likewise the SU(3) $L\sigma M$ $a_0 \to \eta\pi$ decay rate is

$$\Gamma_{L\sigma M}(a_0 \to \eta\pi) = \frac{|\vec{p}|}{8\pi m^2_{a_0}} \left[2g'_{a_0\eta_{NS}\pi} \cos\phi_P\right]^2 \approx 133 \text{ MeV} \tag{29}$$

for $p = 321$ MeV, $g'_{a_0\eta_{NS}\pi} \approx 2.13$ GeV, $\phi_P = 41.84^0$. One may infer a nearby a_0 rate from the PDG tables [6]. Specifically the rate ratio

$$\frac{\Gamma(a_0 \to K\bar{K})}{\Gamma(a_0 \to \eta\pi)} = 0.177 \pm 0.024 \tag{30}$$

and $\Gamma(a_0 \to K\bar{K}) \approx 24.5$ MeV from Refs. [17], then suggests $\Gamma(a_0 \to \eta\pi) \approx 138$ MeV, near Eq. (29). Also, this predicted $L\sigma M$ decay rate (29) is not too distant from the high statistics data [18]

$$\Gamma_{a_0\eta\pi} = (95 \pm 14) \text{ MeV} . \tag{31}$$

The SU(3) companion $f_0(980) \to \pi\pi$ rate is estimated [6] to be

$$\Gamma(f_0\pi\pi) \approx (47 \text{ MeV})(0.781) \approx 37 \text{ MeV} \tag{32}$$

assuming the small $\Gamma(f_0\gamma\gamma) \approx 0.56$ keV rate in the 1998, 1996 PDG tables combined with the measured branching ratio $B(f_0\gamma\gamma) \approx 1.19 \times 10^{-5}$. On the other hand we must account for scalar σ–f_0 mixing (the analogue of pseudoscalar η–η' mixing). Thus in the NS–S basis we define in parallel with Eq. (14)

$$|\sigma\rangle = \cos\phi_S|\sigma_{\rm NS}\rangle - \sin\phi_S|\sigma_{\rm S}\rangle , \quad |f_0\rangle = \sin\phi_S|\sigma_{\rm NS}\rangle + \cos\phi_S|\sigma_{\rm S}\rangle , \tag{33}$$

and estimate ϕ_S from the measured decay rate ratio

$$\frac{\Gamma(f_0\pi\pi)}{\Gamma(a_0\eta\pi)} \approx \frac{3}{2}\left(\frac{470 \text{ MeV}}{321 \text{ MeV}}\right)\left(\frac{\sin\phi_S}{\cos\phi_P}\right)^2 \approx \frac{37 \text{ MeV}}{95 \text{ MeV}} \approx 0.39 \quad \text{or} \quad |\phi_S| \approx 18.3^0 . \tag{34}$$

Prior theoretical estimates were $|\phi_s| \sim 16^0, 20^0$ [12] and 14^0 [19]. The DM2 data of 1989 [6] also suggests from $J/\psi \to \omega\pi\pi$ that $f_0(980)$ is mostly $\bar{s}s$ (not nonstrange), compatible with (34) (and near the ϕ (1020) which is known to be almost all $\bar{s}s$) [12,20].

Lastly we calculate the strong decay rate $\eta' \to \eta\pi\pi$ in the context of the SU(3) $L\sigma M$ [21], with a_0, σ, f_0 poles contributing as $\eta' \to a_0\pi \to \eta\pi\pi$ (4 modes), $\eta' \to \eta\sigma \to \eta\pi\pi, \eta' \to \eta f_0 \to \eta\pi\pi$. Although the $4a_0$ pole modes should dominate, the well–known $L\sigma M$ $\eta' \to \eta\pi\pi$ contact term 3λ [normalized to the quartic term in the SU(2) Lagrangian Eq. (1)] has the opposite sign relative to a_0, σ and f_0 poles and "miraculously cancels" them [22] due to chiral symmetry - assuming one treats the a_0, σ, f_0 poles in narrow width approximation. While Γ_{a_0}/m_{a_0}, $\Gamma_{f_0}/m_{f_0} \sim 1/10$ as needed, the σ is *broad* with $\Gamma_\sigma/m_\sigma \sim 1$.

Then after the chiral cancellation, we must still account for the broad–width σ inverse propagator as $s - m_\sigma^2 + im_\sigma\Gamma_\sigma$ with $|s - m_\sigma^2| << |im_\sigma\Gamma_\sigma|$. Thus the net $\eta' \to \eta\pi^0\pi^0 L\sigma M$ amplitude has the magnitude

$$|M^{\rm net}_{L\sigma M}(\eta' \to \eta\pi^0\pi^0)| \approx |\frac{g'_{\eta'\eta\sigma} g'_{\sigma\pi\pi}}{m_\sigma \Gamma_\sigma}| \approx |\frac{g'_{\eta'\eta\sigma}}{2f_\pi}| \approx 5.7 \ . \tag{35}$$

Here we [11] estimated $g'_{\eta'\eta\sigma} \approx \cos\phi_P \sin\phi_P \, g'_{\sigma\pi\pi} \approx 1.06$ GeV. Then the net SU(3) $L\sigma M$ decay rate is predicted to be (folding in the 3–body phase space integral [23])

$$\Gamma_{L\sigma M}(\eta' \to \eta\pi^0\pi^0) = 1.06 |M^{\rm net}_{L\sigma M}|^2 \text{ keV} \approx 34.4 \text{ keV} \ . \tag{36}$$

A slight increase of this rate (36) is due to the 10% non–narrow widths of the a_0 and f_0 poles. Recent data gives [6] $\Gamma(\eta' \to \eta\pi^0\pi^0) = (42 \pm 4)$ keV. The total decay rate assuming isospin invariance is

$$\begin{aligned} \Gamma_{L\sigma M}(\eta' \to \eta\pi\pi) &\equiv \Gamma_{L\sigma M}(\eta' \to \eta\pi^0\pi^0) + \Gamma_{L\sigma M}(\eta' \to \eta\pi^-\pi^+) \\ &= 3 \times (34.4 \pm 4) \text{ keV} = (103 \pm 12) \text{ keV} \ , \end{aligned} \tag{37}$$

near the total observed rate of $3\times(42\pm4) = (126\pm12$)keV. We know of no other dynamical scheme (such as using the original singlet-octet mixing angles [21]) which recover all the approximately needed SU(3) strong decay rates (27), (29), (36), (37) as found above.

6 Conclusion

In this paper we have consistently avoided dealing with quadratic divergent graphs when computing SU(2) and SU(3) linear σ model ($L\sigma M$) diagrams. Instead in Secs. 2 and

3 we work only with self–consistent log–divergent gap equation integrals Eqs. (4), (10). Sections 3 and 4 extend this pattern from SU(2) to SU(3) dynamical mass-shell equal splitting laws, leading to the off–diagonal eta nonstrange and strange constituent quark masses $m_{\eta_{NS}} \approx 757.9$ MeV and $m_{\eta_S} \approx 801.5$ MeV. Then the dynamical η'–η mixing angle in the NS–S basis is $\phi_P \approx 41.84^0$ compatible with nonperturbative QCD and near many phenomenological analysis of this NS–S angle (see, e.g., Refs. [4,5,13]).

Stated another way, the only SU(3)–breaking pattern we allow is characterized by the constituent quark mass GTR ratio [24] as used in the phenomenological analysis of Refs. [4] $m_s/m \approx 2f_K/f_\pi - 1 \approx 1.44$ for $f_K/f_\pi \approx 1.22$ as measured [6]. Then in Sec. 5 the SU(3) SPP $L\sigma M$ couplings (again following the above MSESLs) of Eqs. (8), (9), (11), (12) in turn predict strong interaction $\sigma_{NS} \to \pi\pi$, $a_0 \to \eta\pi$, $f_0 \to \pi\pi$, $\eta' \to \eta\pi\pi$ decay rates all compatible with data [6].

Acknowledgments: D. Kl. and D. Ke. acknowledge the support of the Croatian Ministry of Science and Technology under the respective contract numbers 119–222 and 009802. M. D. S. is grateful for partial support from the University of Zagreb and for prior conversations with A. Bramon.

Appendix: On the bubble graph integral

If the integrand of Eq. (10) is rewritten using the common denominator $D(x,p^2)$, as $f(x,p^2) \equiv N(x,p^2)/D(x,p^2)$, one should note that the $O(p^6)$ terms in its numerator $N(x,p^2)$ cancel exactly. The numerator is thus a polynomial of degree 2 in (p^2): $N(x,p^2) = c_0(x) + c_1(x)\,p^2 + c_2(x)\,(p^2)^2$. The integrand is therefore conveniently written as the sum

$$f(x,p^2) = \sum_{i=0}^{2} f_i(x,p^2) = \sum_{i=0}^{2} c_i(x)\,\frac{(p^2)^i}{D(x,p^2)}\ . \tag{38}$$

The four–dimensional integral over p is effectively one-dimensional because the integrand depends on p^2 only. After the Wick rotation, we performed this integration analytically, using the *Mathematica* program package. The log–divergent integral $\int d^4p\, f_2(x,p^2)$ depends on our ultraviolet cutoff $\Lambda = 750$ MeV required by Eq. (4). After the p^2–integration, the logarithmic forms

$$l(x) = \ln\left(\frac{m^2 - m^2_{\eta_{NS}}(1-x)x}{m^2 - m^2_{a_0}(1-x)x}\right) \tag{39}$$

appear in the integrand, requiring some care. The mild divergences at the points $x_0 = 0.115698$, $x_1 = 0.222046$, $x_2 = 0.777954$, and $x_3 = 0.884302$ correspond to the roots of polynomials $x \mapsto m^2 - m^2_{\eta_{NS}}(1-x)x$ and $x \mapsto m^2 - m^2_{a_0}(1-x)x$. In order to perform

the residual x integration of the functions $x \mapsto \int d^4p\, f_i(x, p^2)$ $(i = 0, 1, 2)$, the interval $[0, 1]$ is divided into five integration regions, $[0, x_1]$, $[x_1, x_2]$, $[x_2, x_3]$, $[x_3, x_4]$, and $[x_4, 1]$. These integrations were numerical, with an adaptive algorithm which can handle the mild, integrable singularities appearing at the edges of the integration regions.

References

[1] M. Gell–Mann and M. Levy, Nuovo Cimento **16** (1960) 705; see also V. de Alfaro, S. Fubini, G. Furlan, C. Rosetti, Currents in Hadron Physics, Ch. 5, North Holland Amsterdam 1973.

[2] See, e.g., V. Elias and M. D. Scadron, Phys. Rev. **D30** (1984) 647.

[3] R. Delbourgo and M. D. Scadron, Mod. Phys. Lett. **A10** (1995) 251, hep-ph/9910242;
R. Delbourgo, A. A. Rawlinson and M. D. Scadron, ibid, **A13** (1998) 1893, hep-ph/9807505.

[4] A. Bramon and M. D. Scadron, Phys. Lett. **B234** (1990) 346;
A. Bramon, R. Escribano and M. D. Scadron, Eur. Phys. J. **C7** (1999) 271.

[5] T. Feldmann, P. Kroll and B. Stech, Phys. Rev. **D58** (1998) 114006;
T. Feldmann, Int. J. Mod. Phys. **A15** (2000) 159.

[6] Particle Data Group, D. Groom et al., Eur. Phys. J (2000)

[7] A. Salam, Nuovo Cimento **25** (1962) 224; S. Weinberg, Phys. Rev. **130** (1963) 776; for the $Z_3 = Z_4 = 0$ and their $g = 2\pi/\sqrt{N_c}$ compositeness implication, see M. D. Scadron, Phys. Rev. D **57** (1998) 5307.

[8] Y. Nambu and G. Jona-Lasinio, Phys. Rev. **122** (1961) 345.

[9] N. Paver and M. D. Scadron, Nuovo Cimento A78 (1983) 159;
A. Bramon, Riazuddin and M. D. Scadron, J. Phys. **G24** (1998); hep-ph/9709274.

[10] B. W. Lee, Chiral Dynamics, Gordon and Breach 1972, p.12.

[11] D. Kekez, D. Klabučar and M. D. Scadron, J. Phys. G. **26** (2000) 1335; hep-ph/0003234.

[12] M. D. Scadron, Phys. Rev. D26 (1982) 239;
R. Delbourgo and M. D. Scadron, Int. J. Mod. Phys. A **13** (1998) 657;
hep-ph/9807504;
also see N. Paver and M. D. Scadron, Nuovo Cimento **A79** (1984) 57, A81 (1984) 500.

[13] H. F. Jones and M. D. Scadron, Nucl. Phys. **B155** (1979) 409;
M. D. Scadron, Phys. Rev. **D29** (1984) 2076.

[14] D. Klabučar and D. Kekez, Phys. Rev. **D58** (1998) 096003.

[15] P. Ko and S. Rudaz, Phys. Rev. **D50** (1994) 6877.

[16] S. Weinberg, Phys. Rev. Lett. **65** (1990) 1177.

[17] J. A. Oller and E. Oset, Phys. Rev. **D60** (1999) 074023;
A. Astier, Phys. Lett. **B25** (1967) 294.

[18] T. Armstrong et al., Zeit. Phys. **C52** (1991) 389.

[19] M. Napsuciale, "Scalar meson masses and mixing angle in a U(3) $\times$ U(3) linear σ model", hep-ph/9803396.

[20] E. van Beveren et al., Zeit. Phys. **C30** (1986) 615; N. Tornqvist and M. Roos, Phys. Rev. Lett. **76** (1996) 1575; R. Delbourgo, D. Liu and M. D. Scadron, Phys. Lett. **B446** (1999) 332; E. van Beveren, G. Rupp and M. D. Scadron, ibid. **B495** (2000) 300.

[21] J. Schechter and Y. Ueda, Phys. Rev. **D3** (1971) 2871.

[22] pp 324-327 of Currents in Hadron Physics of Refs. [1].

[23] H. Osborn and P. J. Wallace, Nucl. Phys. **B20** (1970) 23;
S.Coon et. al.,Phys. Rev. **D34** (1986) 2784.

[24] Also see A. De Rujula, H. Georgi and S. Glashow, Phys. Rev. **D12** (1975) 147; C. Ayala and A. Bramon, Europhys. Lett. **4** (1987) 777; A. Bramon and M. D. Scadron, Phys. Rev. **D40** (1989) 3779.